AGU PUBLICATIONS

Space Weather

RESEARCH ARTICLE
10.1002/2013SW001008

Key Points:
- The SEPEM application server is a WWW interface to SEP data and models
- SEPEM includes SEP statistical and physical modeling (covers 0.2 AU–1.6 AU)
- SEPEM has integrated effects tools (SEU rate and radiation doses)

Correspondence to:
N. Crosby,
norma.crosby@oma.be

Citation:
Crosby, N., et al. (2015), SEPEM: A tool for statistical modeling the solar energetic particle environment, *Space Weather*, *13*, 406–426, doi:10.1002/2013SW001008.

Received 30 OCT 2013
Accepted 20 APR 2015
Accepted article online 23 APR 2015
Published online 30 JUL 2015

SEPEM: A tool for statistical modeling the solar energetic particle environment

Norma Crosby[1], Daniel Heynderickx[2], Piers Jiggens[3], Angels Aran[4], Blai Sanahuja[4], Pete Truscott[5], Fan Lei[6], Carla Jacobs[7,8], Stefaan Poedts[7], Stephen Gabriel[9], Ingmar Sandberg[10], Alexi Glover[11], and Alain Hilgers[3]

[1]Belgian Institute for Space Aeronomy, Brussels, Belgium, [2]DH Consultancy, Leuven, Belgium, [3]European Space Research and Technology Centre, Noordwijk, Netherlands, [4]Departament d'Astronomia i Meteorologia, Institut de Ciències del Cosmos, Universitat de Barcelona, Barcelona, Spain, [5]Kallisto Consultancy Ltd, Farnborough, UK, [6]RadMod Research, Camberley, UK, [7]Department of Mathematics, CmPA, Catholic University of Leuven, Leuven, Belgium, [8]Now at Space Applications Services NV/SA, Zaventem, Belgium, [9]EEE Group, ECS, University of Southampton, Southampton, England, [10]National Observatory of Athens, Inst. for Astronomy, Astrophysics, Space Applications and Remote Sensing, Athens, Greece, [11]SSA Programme Office, European Space Operations Centre, Darmstadt, Germany

Abstract Solar energetic particle (SEP) events are a serious radiation hazard for spacecraft as well as a severe health risk to humans traveling in space. Indeed, accurate modeling of the SEP environment constitutes a priority requirement for astrophysics and solar system missions and for human exploration in space. The European Space Agency's Solar Energetic Particle Environment Modelling (SEPEM) application server is a World Wide Web interface to a complete set of cross-calibrated data ranging from 1973 to 2013 as well as new SEP engineering models and tools. Both statistical and physical modeling techniques have been included, in order to cover the environment not only at 1 AU but also in the inner heliosphere ranging from 0.2 AU to 1.6 AU using a newly developed physics-based shock-and-particle model to simulate particle flux profiles of gradual SEP events. With SEPEM, SEP peak flux and integrated fluence statistics can be studied, as well as durations of high SEP flux periods. Furthermore, effects tools are also included to allow calculation of single event upset rate and radiation doses for a variety of engineering scenarios.

1. Introduction

Interplanetary space exploration is confronted with many uncertainties specifically in regard to the myriad of energetic charged particles that characterize the space environment [*Crosby et al.*, 2008]. Since the beginning of the space era, space missions have increasingly become more technically sophisticated, while at the same time their sensitivity to the environment that they encounter has also increased. For example, with decreasing feature sizes of modern microelectronics and their use on satellites comes increased sensitivity to single event effects (SEEs) phenomena, instantaneous effects such as single event upsets (SEUs) or "bit-flips," which have become a major concern as a risk to mission success [e.g., *Tretkoff*, 2010]. The Solar Anomalous and Magnetospheric Particle Explorer (SAMPEX) mission was situated in low-Earth orbit with a high inclination and suffered occasional operational anomalies and upsets due to the energetic particles that it was put into space to study [*Baker et al.*, 2012]. Deep-space spacecraft, especially those that target the inner solar system (e.g., MErcury Surface, Space ENvironment, GEochemistry, and Ranging (MESSENGER)) are especially vulnerable to high-energy charged particles [*DiGregorio*, 2008]. Some SEEs are nondestructive and others are destructive. *Dodd and Massengill* [2003] review the physical mechanisms responsible for nondestructive SEEs in digital microelectronics such as SEUs. Electronics on spacecraft usually can survive SEUs by relying on a variety of techniques such as rebooting the on board computer or sending duplicate commands [e.g., *Luo and Zhang*, 2011; *Maris and Crosby*, 2012].

Charged particle radiation is one of the main issues currently being discussed in regard to sending humans on long-term interplanetary missions (e.g., return trip to Mars) [*Cucinotta et al.*, 2010]. It is well known that the galactic cosmic ray (GCR) flux in the solar system is modulated by solar activity, and as a first approximation, the GCR background intensity can be said to be slowly varying and therefore predictable over short

timescales (highest at solar minimum and lowest at solar maximum). Due to their high energies (0.1–1000 GeV), of which the 100 to 1000 MeV fluxes constitute the largest contribution, GCRs represent the most significant hazard for long-term missions in interplanetary space because manned spacecraft are usually heavily shielded resulting in an increased risk of secondary radiation. During the recent solar minimum, the measured intensities of major species from C to Fe, measured by the Advanced Composition Explorer (ACE) spacecraft, were each 20%–26% greater in late 2009 than in the 1997–1998 minimum and previous solar minima of the space age [*Mewaldt et al.*, 2010], suggesting that current GCR empirical models may be underestimating the true nature of the GCR background. The Badhwar-O'Neill GCR model has been revised to model all balloon and satellite GCR measurements since 1955 including these new ACE measurements [*O'Neill*, 2010].

On the other hand, large solar energetic particle (SEP) events have a greater occurrence probability about the solar maximum period than about the minimum being, as they are, a phenomenon associated with solar flares and shock waves driven by coronal mass ejections (CMEs). Extreme SEP events (such as those in January 2005 and December 2006) have been known to occur during the declining phase of the solar cycle [*Crosby*, 2009]. SEP events are mainly composed of protons, electrons, and α particles with small contributions of ^{3}He nuclei and heavier ions up to iron. There have been observations of ultraheavy ions [e.g., *Mason et al.*, 2004]. Such SEP events are sporadic with energies from tens of keV to a few GeV and may last from a period of hours to days or even weeks (depending on the energy of interest). While predicting hazardous SEP events well in advance remains the ultimate goal, we currently rely on short-term predictive capabilities based on ground-based observations (neutron monitors), space-based in situ observations at L1 (shock arrival and energetic storm particles), and remote sensing (solar flares, CMEs, and active regions), as well as theoretical understanding (models), [e.g., *Luhmann et al.*, 2010; *Vainio et al.*, 2009; *Rodríguez-Gasén et al.*, 2014]. Protons in the $>$10 MeV energy range are important contributors to ionization, displacement damage, and sensor background; while protons below 10 MeV are the main contributors to displacement damage in solar cells [see, for example, *Feynman and Gabriel,* 2000]. A 10 MeV proton may only penetrate ~0.6 mm aluminum shielding, but a 30 MeV proton can penetrate over 4 mm making protons in the energy range from a few MeV to hundreds of MeV important despite the relative steepness of SEP energy spectra. As a result, SEP events are a serious radiation hazard concern for both spacecraft and humans traveling in space. For the assessment of human extravehicular activities (EVAs) during SEP events energies greater than 10 MeV are monitored; the impacts of extreme SEP events on humans were investigated by *Jiggens et al.* [2014].

Understanding of the SEP radiation environment is steadily improving due to the long-term SEP data sets that have been acquired during the last decades as well as the scientific advances that have been made in the underlying physics behind the generation mechanism of SEP events. This acquired knowledge provides the community with the opportunity to review and update existing statistical models of the dynamic SEP environment based on near-Earth data sets. On the other hand, interplanetary SEP in situ observations at heliocentric distances away from 1 AU are sparse when compared to near-Earth (1 AU) data sets. Hence, to perform statistical modeling of the SEP environment away from a heliocentric distance of 1 AU requires alternative approaches such as the building of synthetic data sets using physics-based models for data assimilation.

Bearing the above in mind, the main incentive behind the European Space Agency (ESA) Solar Energetic Particle Environment Modelling (SEPEM) project that ended in 2013 was to create new SEP engineering models and tools while addressing current and future needs of the user community. In order to allow the community access to the spacecraft data and the models that were implemented as well as established modeling practices, the SEPEM application server was developed. The server is a WWW interface to SEP data and a range of modeling tools and functionalities intended to support space mission design (see left side menu in Figure 1 for an overview). Background material, information on the data sets and processing, and context sensitive help for each application page are also available (Figure 1, right hand menu). Recently, the SEPEM application server was updated and it now includes SEP modeling at heliocentric distances ranging from 0.2 to 1.6 AU. This paper presents the main outcomes of the SEPEM project including the data processing tools, creation of the SEPEM reference proton data set, the event list tool, statistical and physics-based modeling tools, effects tools, and the SEPEM application server.

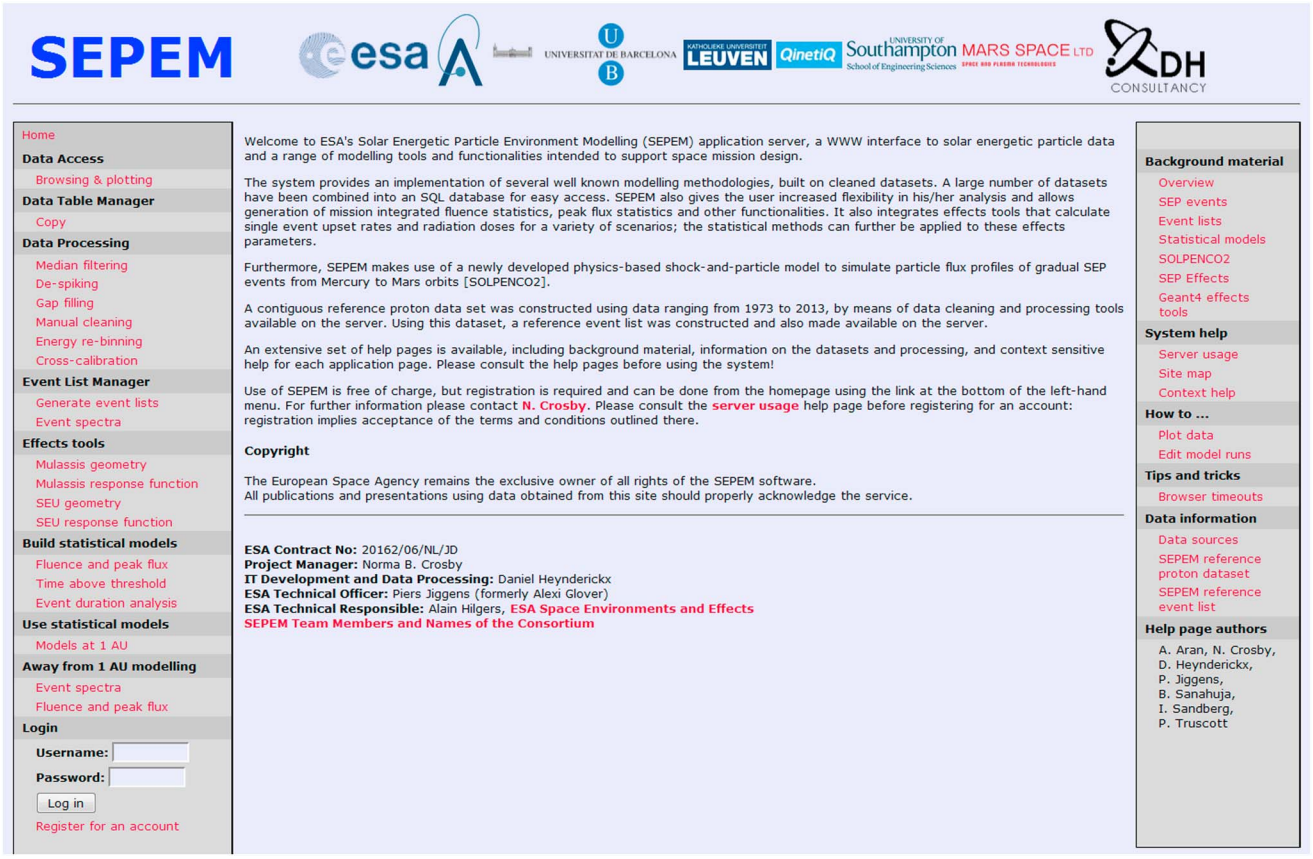

Figure 1. The SEPEM application server with its WWW interface to SEP data and a range of (left side menu) modeling tools and functionalities and (right side menu) background material.

2. The SEPEM Reference Proton Data Set and Event Lists

To be able to perform useful statistical analyses on SEP events implies having a data set spanning as many solar cycles as possible. It is also important that the data set is contiguous, uniform, and of high quality. The impact of limited length and quality of data sets on SEP models was previously investigated [*Rosenqvist and Hilgers*, 2003; *Rosenqvist et al.*, 2005; *Glover et al.*, 2008]. In order to provide the facility for reliable statistical modeling capability, the SEPEM reference proton data set was created based on Geostationary Operational Environmental Satellite (GOES) 5, GOES 7, GOES 8, GOES 11/Space Environment Monitor (SEM) data [*Onsager et al.*, 1996; *Sellers and Hanser*, 1996], GOES 13/Energetic Particles Sensor (EPS) data [*Rodriguez et al.*, 2014], and Interplanetary Monitoring Platform 8 (IMP 8)/Goddard Medium Energy (GME) data [*McGuire et al.*, 1986]. The data set has been generated taking into account known data caveats and represents the "best effort" data set that could be generated based on the information retrieved from instrument teams and a complete literature search.

The SEPEM reference proton data set ranges from 1973 to 2013 and is composed of 10 reference energy channels exponentially distributed in range from 5 to 200 MeV (5.00–7.23 MeV, 7.23–10.46 MeV, 10.46–15.12 MeV, 15.12–21.87 MeV, 21.87–31.62 MeV, 31.62–45.73 MeV, 45.73–66.13 MeV, 66.13–95.64 MeV, 95.64–138.3 MeV, and 138.3–200.0 MeV). Building the data set was a two-step process. First, the data sets were processed by removing data spikes and periods where problems such as saturation, pulse pileup, contamination, etc. occur, and filling in data gaps (including gaps introduced by removing bad data).

It should be noted that only data spikes were removed from the GOES data, there is no evidence of saturation or similar effects. There are a small number of short (hours or less) gaps in the GOES data during events, both in the original data and by removing data spikes. These gaps were filled by performing a linear interpolation between the last and first flux (not log flux) values before and after the gaps, as a

function of time. Each time, the data from the secondary GOES spacecraft and from IMP 8/GME where available, were checked to make sure that no short-term features were missed. In the background regime (i.e., outside of event periods), the number of gaps is much larger, but they mostly manifest themselves as intermittent dropouts, not as continuous periods of missing data. These gaps were filled as well, using the same procedure. The gap-filling procedure can be evaluated by comparing the original data sets with the processed ones, both being available in the system. In addition, the data cleaning and gap filling tools are available as well.

The IMP 8/GME data exhibit much more severe gaps, especially after removing the bad data points. This behavior gradually worsens with time, and the problem of gap filling becomes insurmountable after 1984 when GOES data become available. Hence, it was decided to only clean the GME data and not attempt to fill in the data gaps. This implies that for the period 1973–1983 the data exhibit small gaps even during events. From 1984 on, the data set is based on GOES data and is continuous; for this period, the GME data were only used to cross calibrate the GOES data.

After correcting and completing the data and prior to cross calibration, there still remained the issue of differences in the energy channels between different instruments, so the data cannot easily be combined. This required additional processing of the data: rebinning of the individual data point spectra into a reference energy spectrum, cross calibration of the rebinned data, and merging of the individual data sets without overlaps in time.

Energy rebinning was done point by point using a piecewise power law to interpolate between the two closest energies in the processed data of both GOES/SEM and EPS and IMP 8/GME. The instruments on the GOES spacecraft were built for monitoring purposes and, as a consequence, exhibit significant differences in response as they were not rigorously calibrated. On the other hand, the IMP 8/GME instrument is a science quality instrument and was therefore properly calibrated. In SEPEM the procedure adopted was to use the common baseline of IMP 8/GME to cross calibrate the instruments on the GOES spacecraft using only points in time for which there was data in both data sets after the removal of bad data points. This is allowed for the exploitation of the best facets of SEM and EPS and GME, namely, consistent data coverage without dead time or saturation and high-energy resolution, respectively, in the creation of the SEPEM proton reference data set. As a result of this cross calibration, the background level was reduced and thereafter found to be negligible during SEP events (background subtraction not necessary). The SEPEM reference proton data set is thus composed of the following: (1) IMP 8/GME data from 1973 up to 1984: bad data points removed, no gap filling performed, and (2) GOES/SEM and EPS data from 1984 up to 2013: data spikes removed, all gaps filled.

The GOES/SEM and EPS proton fluxes were scaled to the IMP 8/GME data which has better energy resolution. The time resolution of the SEPEM proton reference data set is 30 min prior to 1984 (based on the IMP 8/GME data) and 5 min from 1984 onward (based on the GOES/SEM and EPS data series). More information about the SEPEM reference data set construction can be found in *Jiggens et al.* [2012] and on the SEPEM application server [http://dev.sepem.oma.be/]. Based on recent data processing work by *Sandberg et al.* [2014], it is planned to upgrade the current data processing chain in the future.

As part of ongoing work, the GOES data prior to 1984 are being recovered and processed: the GOES (and precursor Synchronous Meteorological Satellite (SMS)) mission started to deliver data in 1974, but these data have never been processed into the ASCII format used for the later GOES data sets. One of the authors (D. Heynderickx) has processed the old Flexible Image Transport System (FITS) file data set and converted it into ASCII format. These data are now also being processed (spike removal and gap filling) to extend the coverage of the GOES data down to 1974 (an extra solar cycle); in fact, the 1984–1986 GOES 5 data in the SEPEM database were already recovered from these old files. When the laborious procedure of processing these data is complete, SEPEM will contain a continuous GOES data set from 1974 up to present. The reference data set will then consist of GOES data only, calibrated using GME data such that it is reliable and homogenous.

The data processing tools that were used to build the reference data set (manual cleaning, gap filling, energy rebinning, and cross calibration) and others (median filtering and automatic despiking) are available on the SEPEM application server. The user also has access to all data sets including raw and cleaned that have been combined into a Structured Query Language (SQL) database with easy access through the application server.

Table 1. Overview of the Particle Data Sets (Proton (p^+), Electron (e^-), He, Heavier Ions) That Are Available on the SEPEM Application Server[a]

Spacecraft	Detector	Particle
SMS 1, SMS 2	SEM	p^+, e^-
GOES 1, GOES 2, GOES 3, GOES 5, GOES 6, GOES 7, GOES 8, GOES 9, GOES 10, GOES 11, GOES 12, GOES 13	SEM	p^+, e^-
IMP 8	GME	p^+, He, e^-
IMP 8	CPME	p^+, He, e^-, ions
ACE	EPAM	ions, e^-, He, O, Fe
ACE	SEPICA	H, He, C, O, Ne, Mg, Si, Fe
ACE	SIS	He, C, N, O, Ne, Na, Mg, Al, Si, S, Ar, Ca, Fe, Ni
ACE	ULEIS	ions, H, He, C, O, Fe
HELIOS 1	E7 Trainor	p^+
HELIOS 2	E7 Trainor	p^+

[a]More information about these data sets can be found online: http://dev.sepem.oma.be/help/data_sources.html.

Table 1 lists the available raw particle (proton, electron, He, and heavy ions) data sets (for more details see http://dev.sepem.oma.be/). Energy ranges of the various particle data sets can be found when using the "browsing and plotting" function available on the application server. At present, the proton data have been carefully processed, and work to process the heavy ion data is underway in a follow-on ESA activity. The methods of data processing are broadly available on the system to ensure that the steps are reproducible. However, a full list of manually removed spikes is not presently included online and it is planned to investigate replacing this operation with an automatic one to improve reproducibility. Furthermore, there is presently no method on the SEPEM system for merging data sets sequential in time, the inclusion of this functionality is being investigated (the reference data set was merged manually).

Each module in such a system has its own associated errors, and propagating these errors through combined operations is not straightforward and may require a huge amount of processing time. Methods for estimating data, modeling, and combined errors are being investigated in ongoing activities to update the SEPEM system.

The SEPEM system was designed including tools available to users to create event lists appropriate for their analyses. Six parameters are available to the user to produce their event list: start threshold, end threshold, minimum peak value, minimum duration, dwell time, and extension. The standard method in literature to define events is to select thresholds/peak values based on particle fluxes, however, additionally in SEPEM these can even be created using thresholds of effects parameters such as ionizing dose. The dwell time parameter allows for the combination of any enhancements separated by less than the selected time value so that they are treated as the same event in the list. This can be important for statistical models as such enhancements are likely to be interdependent in both occurrence and magnitude [*Gopalswamy et al.*, 2003] and treating them as separate events would result in the model systematically underpredicting the likelihood of consecutive flux enhancements [*Feynman et al.*, 1990; *Tylka et al.*, 1997b]. However, for other users, such as those interested in the characteristics of separate enhancements, a dwell time of zero may be appropriate. Similarly, the extension value allows for a user-defined extension either side of the event if the user is concerned about missing significant SEPs as a result of their choice of energy channel and flux thresholds.

For users who are not interested in creating their own event list and in order to produce a new set of statistical models, a SEPEM reference proton event list at 1 AU was created covering the time span of the SEPEM reference proton data set (1973 to 2013). The 7.23–10.46 MeV proton channel was selected as the reference channel for defining events, the justification is twofold; it ensured that all periods where there were significant flux increases resulting from solar origin in any channel were detected, while on the other hand the energy range was high enough to be certain that none of the increases were the result of trapped radiation or electron contamination. The start threshold of an event was defined as when the flux in the SEPEM reference proton energy channel (7.23–10.46 MeV) went above 0.01 $cm^{-2}\,s^{-1}\,sr^{-1}\,MeV^{-1}$ and the end threshold of the event as when the flux returned to this value. It is the quality of the cleaned data that allows for this low start/end event threshold, minimizing the chance of missing high-energy particles, a significant portion of which can arrive earlier than the point in time the 7.23–10.46 MeV proton flux reaches higher levels [*Jiggens et al.*, 2012]. Due to some remaining background noise (e.g., noneruptive phenomena and instrumental), many small

enhancements not of solar origin were detected. To compensate for this, a minimum event duration of 24 h was chosen and a minimum peak flux of 0.5 $cm^{-2}\,s^{-1}\,sr^{-1}\,MeV^{-1}$ (in the reference proton energy channel) was introduced to remove erroneous and insignificant events. Furthermore, a dwell time of 24 h between events was set based on a visual investigation into the origins of enhancements separated by 6, 12, 24, and 48 h. The value of 24 h was found to minimize occurrence of grouping of nonrelated events while grouping those events that were clearly connected. Events coming from the same active region are not statistically independent compared to those coming from different active regions, and while these solar events are often separated by more than 24 h the SEP enhancement as seen at 1 AU is not. The correct choice of such a threshold for producing an event list for statistical modeling is strongly dependent on the reference energy channel and the flux thresholds selected. A comparison of usage of different event lists applied to widely used statistical models is available on the system help pages: http://dev.sepem.oma.be/help/sepe_lists.html.

The current SEPEM reference proton event list is available on the SEPEM application server and includes 250 events. Figure 2 (top) shows the proton flux time profiles of the 10 SEPEM energy channels for the SEPEM reference proton event that began on 5 March 2012. For comparison, Figure 2 (bottom) shows the ACE Electron, Proton, and Alpha Monitor (EPAM) electron, He, O, and Fe flux profiles for the same event. It is possible for the user to retrieve the data used to produce the plots in ASCII format.

A functionality on the server allows the user to compute energy spectra for both the peak flux and the total fluence of an event for a selected particle species. An option is available to superimpose spectrum fits (power law in energy, exponential in energy, and exponential in rigidity) on the spectrum plots. Peak flux spectra of an event consist of the maximum values encountered during each event for each channel individually (not necessarily coincident in time). Total fluence spectra are generated by summing the instantaneous flux values for each data record, multiplied by the time in seconds, between the start and end times of each event, for each channel separately. It is planned to include more complex functional forms such as Band fits [*Band et al.,* 1993; *Mewaldt et al.,* 2005] in the future.

3. Radiation Effects Analysis Tools

High-energy solar protons are one of the major sources of ionizing radiation damage to spacecraft. They can have detrimental effects on microelectronics, sensors, and solar cells used in space systems, as well as cause damage to materials and biological cells. A balanced approach has therefore to be taken to apply the range of radiation mitigation measures (such as shielding, component selection/hardening, operational changes) to protect the crew and hardware (exterior and interior) from the radiation environment encountered in space. Modeling the effects of energetic particle radiation is one of the key challenges in spacecraft design. Research into SEEs has mostly relied on prelaunch testing of components. However, the true measure of any ground test methodology is how closely results agree with flight data. Indeed, a key parameter for determining the probability of SEEs occurring is the incident particle spectra from the environment. This latter approach provides spacecraft designers and operators with more realistic information about the true nature of the space environment that will be encountered.

For this purpose, SEPEM has integrated radiation effects analysis tools to allow the calculation of total ionizing dose by SEPs, shielded particle fluxes, and SEU rates for a variety of engineering scenarios. Calculations are performed using the MULti-LAyered Shielding SImulation Software (MULASSIS) [*Lei et al.*, 2002] and the GEant4-based Microdosimetry Analysis Tool (GEMAT) [*Lei*, 2007; *Lei and Truscott*, 2007]; both tools are based on the Geant4 [*Agostinelli et al.*, 2003; *Allison et al.*, 2006; http://geant4.web.cern.ch/geant4/; http://geant4.esa.int/] radiation transport simulation toolkit. The calculation of total ionizing dose and shielded fluxes resulting from incident SEPs is provided by MULASSIS as a function of shielding [*Lei et al.*, 2002]. SEU rates from the shielded ion flux are calculated based on the Linear Energy Transfer (LET) spectrum and path length distribution method, with user supplied device geometry and upset cross sections. For ions heavier than protons ($Z \geq 2$), the calculation is a derivative of the Integrated Rectangular Parallelepiped method [*Petersen*, 1997; *ECSS-E-HB-10-12A*, 2010]. Here GEMAT computes the path length distribution of the given geometry [*Lei*, 2007; *Lei and Truscott*, 2007], and another tool converts the shielded particle fluxes to LET spectra based on proton and heavier ion stopping powers in silicon [*International Commission on Radiation Units and Measurements (ICRU)*, 2005; *Sigmund et al.*, 2009; Ziegler et al., http://www.srim.org]. For predicting SEU rates due to protons, the proton SEU cross section is integrated over the shielded proton flux.

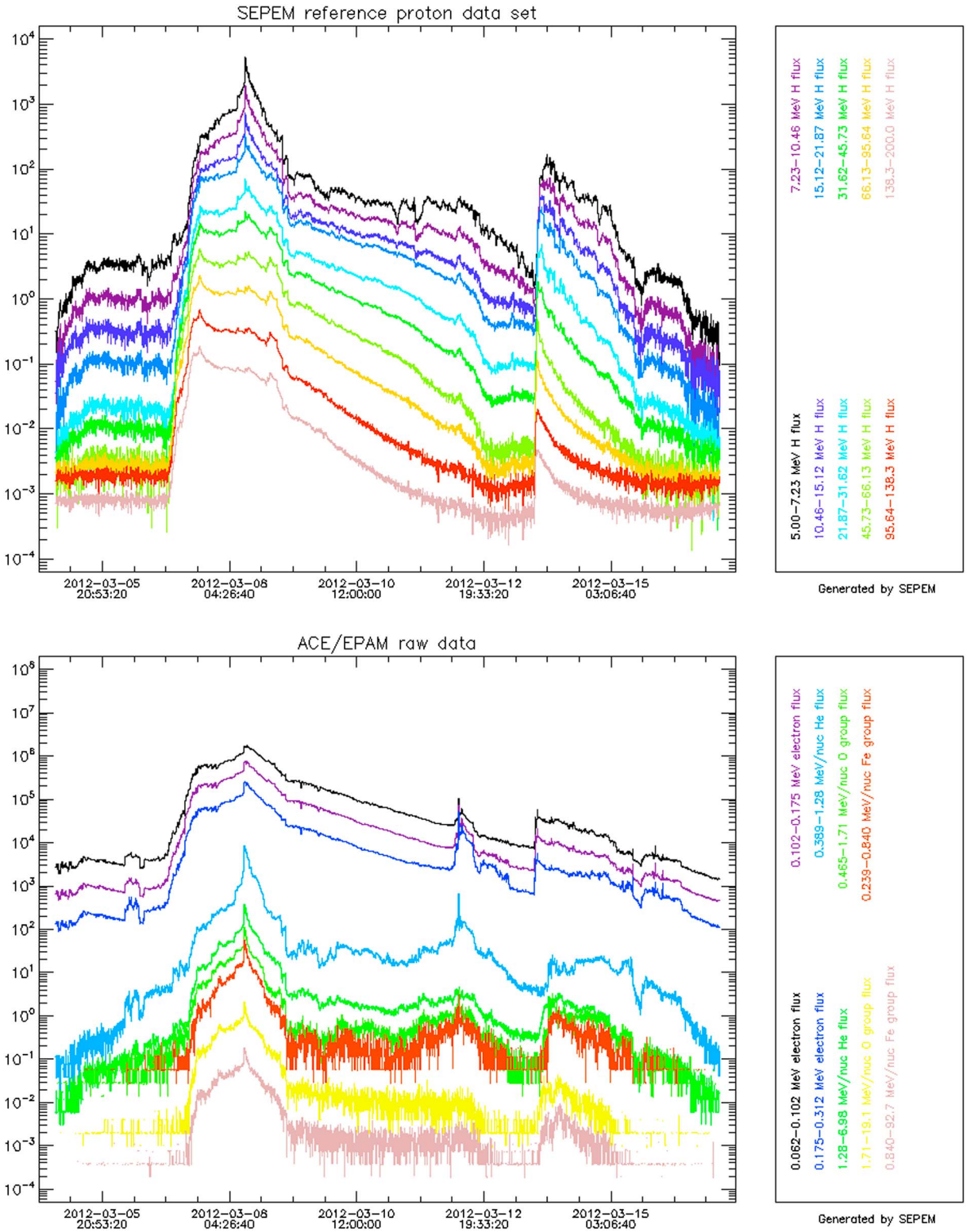

Figure 2. (top) Proton flux profiles for the duration of the SEP SEPEM reference proton event that began on 5 March 2012 00:30:00 and ended on 17 March 2012 02:25:00 in the 10 SEPEM reference energy channels. (bottom) Electron, He, O, Fe flux profiles as observed by EPAM on board the ACE spacecraft for the same SEP event.

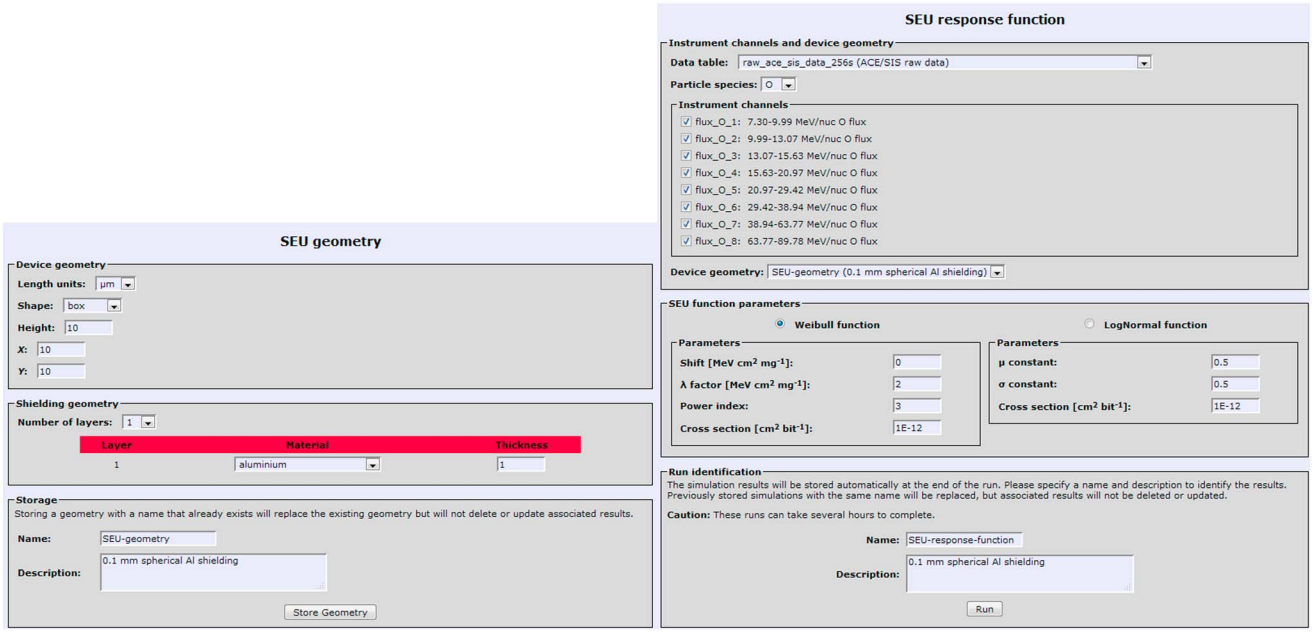

Figure 3. The (left) SEU geometry interface and the (right) SEU response function interface.

To use these tools in SEPEM, little knowledge of Geant4 is necessary and the user only has to define the data table, the particle species, the device geometry, and the device upset cross-section parameters. An example of a SEU rate computation is given to illustrate the usage of these functionalities. The geometry is defined by selecting "SEU geometry" (see under "Effects Tools" in Figure 1) and filling in the form (Figure 3, left). In this example, a cubical device with a single-layer Al spherical shielding is selected and the geometry is stored by clicking on the "Store Geometry" button. The response function is then computed by selecting the "SEU response function" and by filling in the form (Figure 3, right). In this example, the ACE Solar Isotope Spectrometer (SIS) oxygen data set is utilized as well as the simple box geometry that was defined. Figure 4 (left) shows the path length distribution in the device in units of events/bin per incident particle, and the corresponding SEU rate during the SEP event (oxygen data) that began on 5 March 2012 is shown in Figure 4 (right). The current version of SEPEM is only able to treat one particle species at a time, while for the true upset rate one needs to combine the LET spectra from multiple ions (this functionality is presently under development). SEPEM statistical methods that are described in section 4 can also be applied to these effects parameters.

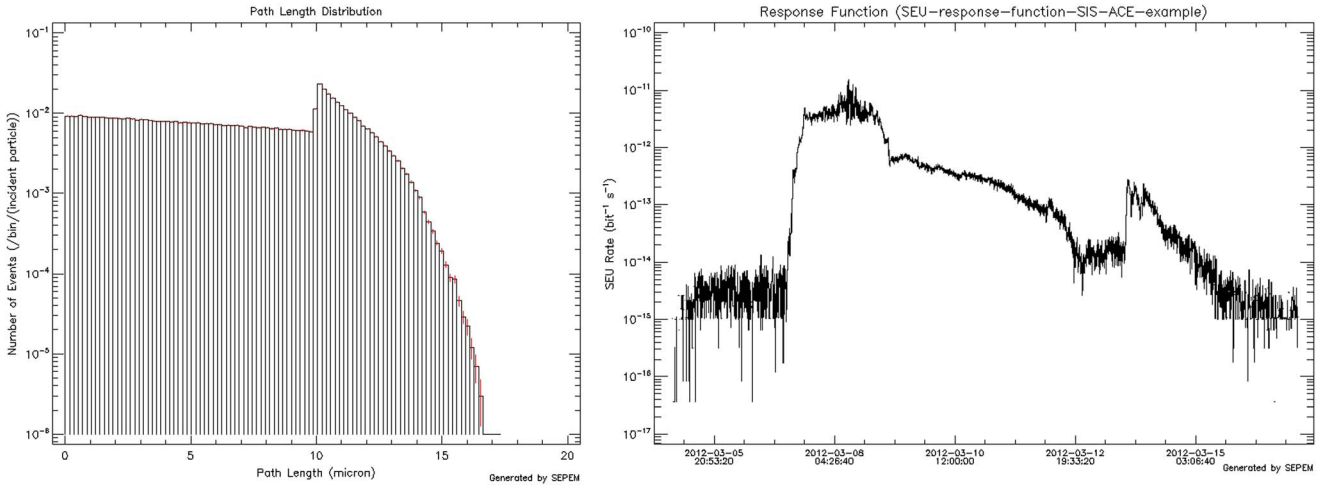

Figure 4. (left) Path length distribution in the device in units of events/bin per incident particle. (right) Corresponding SEU rate during the SEP event (oxygen data) that began on 5 March 2012.

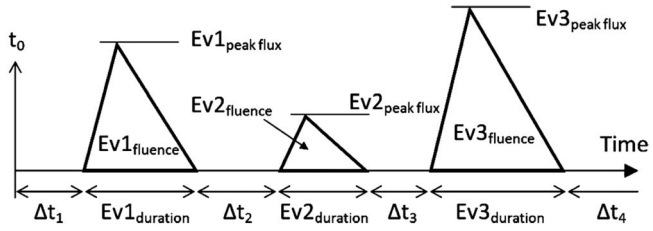

Figure 5. Cartoon representing the Virtual Timeline method. Courtesy of *Jiggens et al.* [2012].

4. Statistical Tools

In order to assist spacecraft designers mitigate the effects of SEPs, statistical models are built for the description of the SEP environment. These models provide predictions of a given SEP parameter (e.g., peak flux and cumulative fluence) over a user-specified mission duration as a function of confidence level. To produce probability curves, the SEPEM application server hosts well-known statistical methods such as the Monte Carlo method (similar to the Jet Propulsion Laboratory (JPL) model) [*Feynman et al.*, 1990, 1993, 2002; *Rosenqvist et al.*, 2005; *Glover et al.*, 2008] and the Emission of Solar Proton (ESP) methods: worst case [*Xapsos et al.*, 1998, 1999] and cumulative [*Xapsos et al.*, 2000]. The empirical JPL model is based on a continuous record of daily average $>$1, 4, 10, 30, 60 MeV proton fluxes and on the separation of the solar cycle (11 years) into active periods (2.5 years before and 4.5 years after solar maximum) and quiet periods (4 years). The contributions from quiet years are not considered in the model as they are considered negligible compared to those from the active years. Similar to the JPL model, the same assumption (only active years) is considered in the ESP models, though a data-driven solar minimum model is included in the later Prediction of Solar particle Yields for CHaracterizing Integrated Circuits (PSYCHIC) paper [*Xapsos et al.*, 2004]. The proton flux energy range used in the ESP models extends from $>$1 MeV to $>$300 MeV, and the models use maximum entropy theory that provides a mathematical procedure to select the least biased distribution, subject to constraints imposed by available information.

Both the JPL and the ESP methods use the Poisson distribution to model the occurrence of SEP events, although the way in which they do so varies. Differences between these two methods are discussed in *Jiggens et al.* [2012]. The application of this distribution is reasonable (although perhaps not always accurate) in SEP environment models only for solar active years during which most of the solar fluence is contained. Recent extreme SEP events (e.g., January 2005 and December 2006) occurring during the declining phase of the solar cycle suggest that for studying continuous data sets covering several solar cycles other distributions should be considered.

A new statistical method entitled "Virtual Timelines" was developed under the SEPEM project and allows for a more realistic representation of the environment. In this new method, the distribution of waiting times (defined as the time from the end of one event to the onset of the following event) is used as opposed to the event frequency [*Jiggens et al.*, 2012]. The system includes time-dependent Poisson and Lévy distributions [*Jiggens and Gabriel*, 2009] as options for users to model the distribution of SEP events in time in addition to the traditional Poisson distribution (which assumes events are randomly distributed in time). The virtual timelines method allows for the consideration of nonnegligible event durations fit with the same procedure as the waiting times meaning the system can produce event duration and time above a threshold outputs. This also allows the model to remain applicable for shorter mission (or mission phase) durations for flux calculations by use of numerical regression to the event peak flux or fluence characteristics as, in such cases, event-to-event variations in duration are important whereas for longer duration models they may even out. The system provides the same choice of three distributions for fitting durations as for waiting times. The timelines are created with waiting times interspersed with events and their associated durations [*Jiggens et al.*, 2012]. Figure 5 represents a cartoon of the Virtual Timeline methodology where Δtn is the waiting time prior to event Evn with peak flux, $EVn_{peak\ flux}$, and fluence, $EVn_{fluence}$. Solar quiet and active periods can be treated separately as per the JPL formulism or combined.

The system allows the user to run different models on the same data set and, therefore, determine the differences in outputs coming from the models themselves distinct from the underlying data used to generate them. Figure 6 compares the mission fluence for the three methods (JPL, ESP, and Virtual Timeline) for two mission durations (1 year and 7 years) using the same (SEPEM reference) data set.

Table 2 lists the four SEP statistical methods that are available on the SEPEM application server: Monte Carlo (JPL method), Worst-case ESP method, Cumulative ESP method, and Virtual timelines. SEP parameters

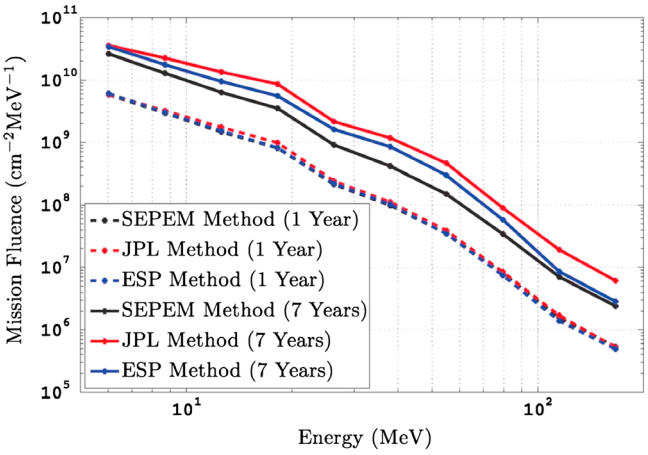

Figure 6. Comparison of methods for mission cumulative fluence spectra with 90% confidence level using the SEPEM proton reference data set. Courtesy of *Jiggens et al.* [2012].

(Fluence, Peak Flux, Event duration, and Time above threshold) that the methods can be applied to are also identified in the table. The statistical models can be run by selecting one of the model types (fluence and peak flux modeling, time above threshold, and event duration) listed under "Build statistical models" (Figure 1, left hand menu). As an example "Fluence and peak flux modeling" has been chosen. Once selected, the relevant form is displayed (Figure 7, top). The SEPEM reference data set and event list have been selected, and the form expands (Figure 7, bottom). In this example, the fluence is chosen as the parameter and the JPL method is utilized. Six default mission lengths ranging from 0.5 to 7 years are identified and can be changed by the user. Once the fields have been filled in, the process can be run. To interpret, the results of the run various plot files (distribution functions, probability curves, duration fits, and waiting time fits) can be retrieved.

In Figure 8, some examples are shown. In Figure 8 (top left), the three fluence distribution function fits (lognormal, truncated power law, and cutoff power law) are compared to the data (black); and in Figure 8 (top right) the differences between the logarithms of the sample data in the event list and the three flux distribution fits are shown. Figure 8 (bottom left) displays the probability of exceeding the predicted cumulative mission integrated value for mission lengths ranging from 0.5 year to 7 years (default values); and in Figure 8 (bottom right), the probability of exceeding the predicted worst-case event fluence value for the identified seven mission lengths is shown based on the distribution chosen (in this case the cutoff power law). The user may choose between the different possibilities available on the SEPEM system. For a comparison of the statistical model distribution fits as well as the resulting outputs, see *Jiggens et al.* [2012].

In addition to the *fluence and peak flux* models, the SEPEM system also allows the user to perform *time above threshold* and *event duration analysis* modeling providing outputs as a series of curves of the model parameter as a function of mission length, for each confidence level. The event duration analysis is run on a user-defined event list and provides cumulative and worst-case outputs. For these models, a fit is needed for the distribution of event durations defined by the event list threshold parameter; the same choices as for the distribution of SEP events in time are available (although one should consider that as the outputs are in the time domain, the distribution fitted is the Fourier transform of the probability density function). A high dwell time or low-minimum event duration might not be appropriate for this type of analysis.

The time above threshold models are simplified and created directly from the chosen data set using only a single parameter of threshold. In Figure 9 (left), the probability of exceeding the selected proton threshold

Table 2. SEP Statistical Methods Available on the SEPEM Application Server and Parameters That the Methods Can Be Applied to

	SEP Parameter			
Methods	Fluence Analysis	Peak Flux Analysis	Duration Analysis	Time Above Threshold
Monte Carlo (JPL method)	X	X		
Worst-case ESP method	X	X		
Cumulative ESP method	X			
Virtual timelines	X	X	X	X

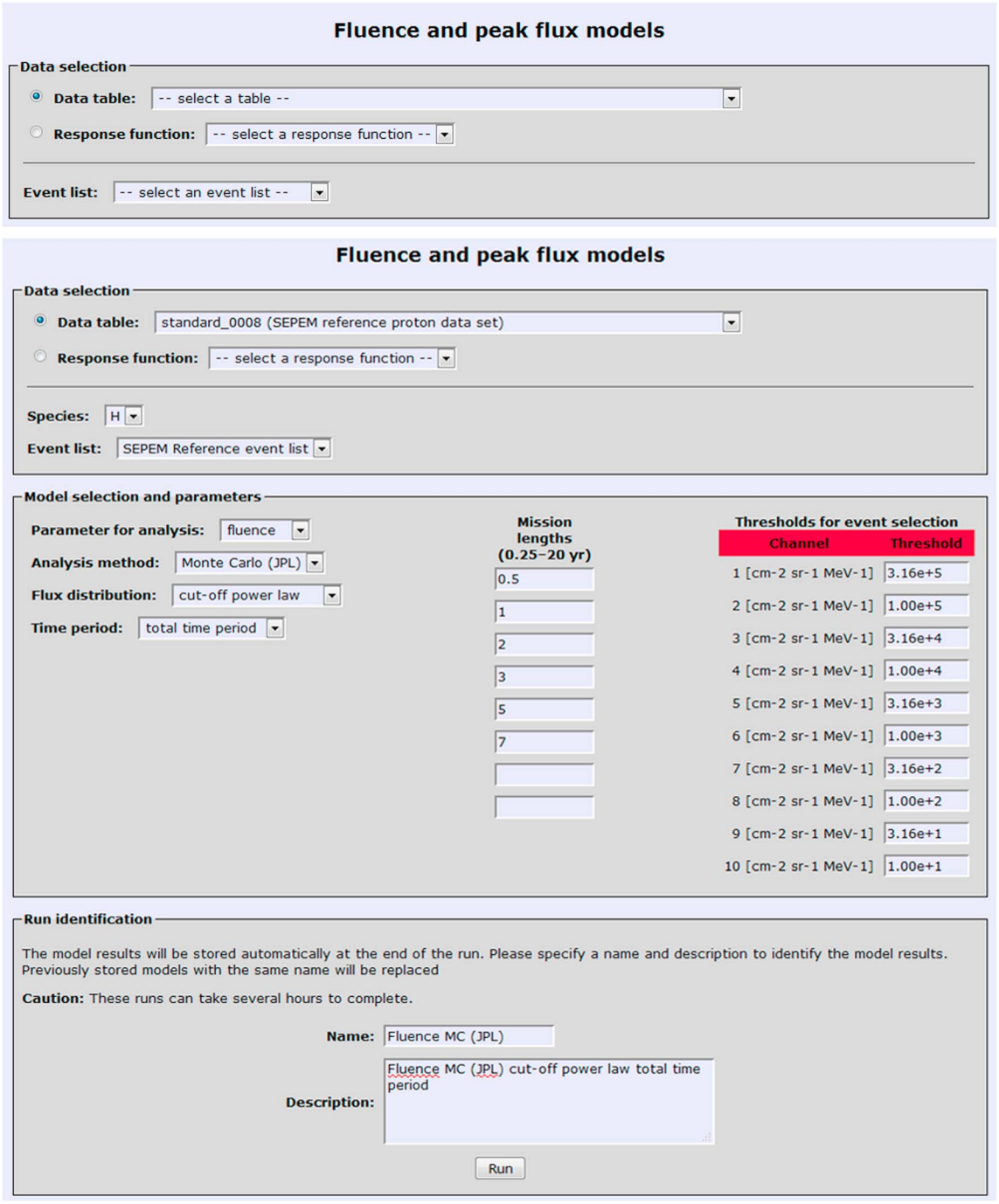

Figure 7. (top and bottom) Example of a filled in "Fluence and peak flux" form using the SEPEM application server.

value, 15.80 $cm^{-2}\,s^{-1}\,sr^{-1}\,MeV^{-1}$, based on the second channel in the SEPEM reference data set as a function of total time above threshold is shown for six mission lengths. The duration above the selected threshold value, 15.80 $cm^{-2}\,s^{-1}\,sr^{-1}\,MeV^{-1}$, for various confidence levels as a function of mission length is shown in Figure 9 (right).

In a separate page entitled *Models at 1 AU* (see Figure 10, top), energy spectra parameterized by confidence level can be produced, and proton fluxes and fluences can be scaled to ion fluences using abundance tables based on the Cosmic Ray Effects on Micro-Electronics 96 (CREME96) 5 min worst-case peak

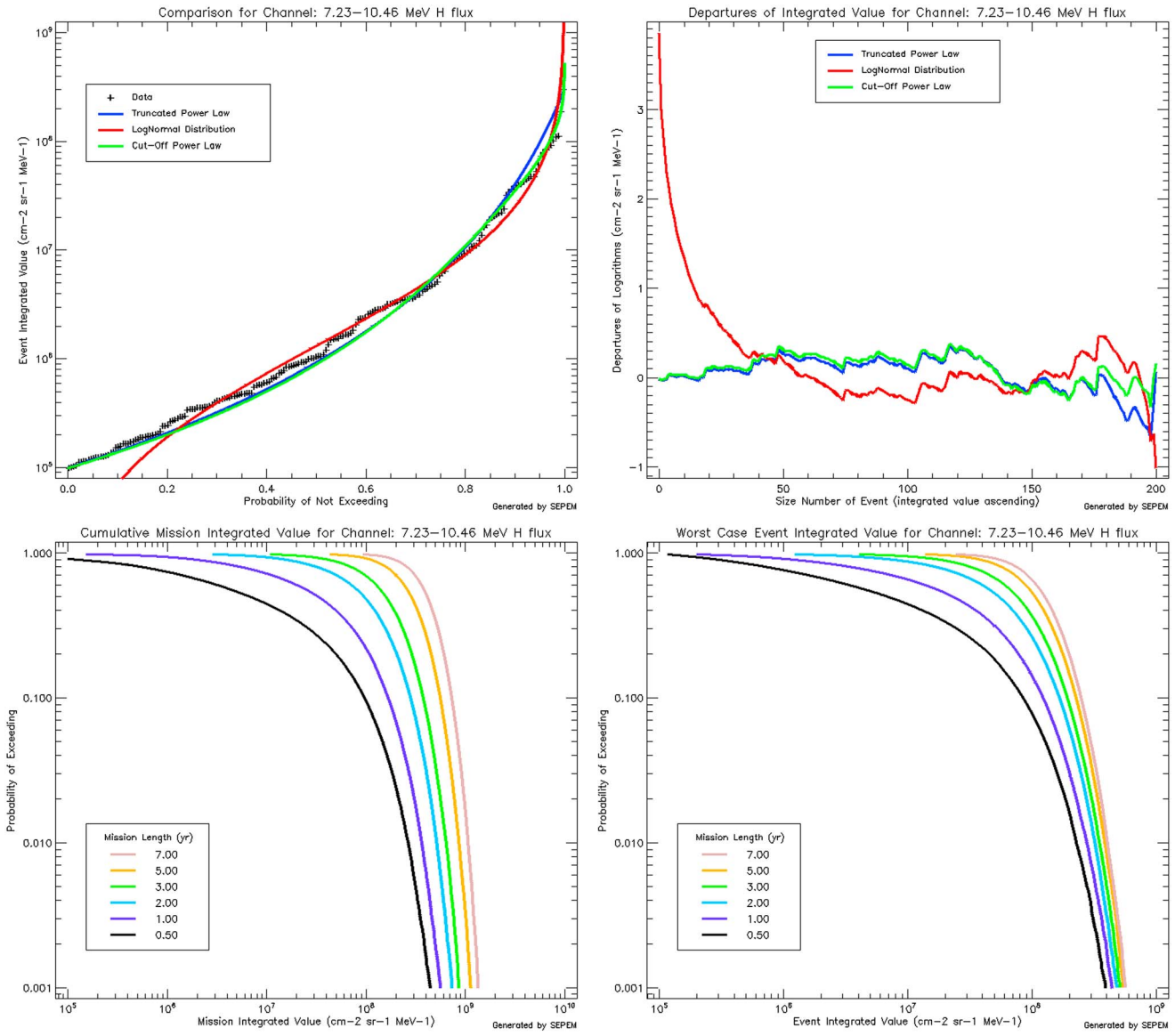

Figure 8. Results refer to the 7.23–10.46 MeV energy channel. (top left) The three distribution function fits (lognormal, truncated power law, and cutoff power law) are compared to the data (black). (top right) Differences between the logarithms of the sample data in the event list and the three flux distribution fits are shown. (bottom left) The probability of exceeding the predicted cumulative mission integrated value for mission lengths ranging from 0.5 to 7 years. (bottom right) The probability of exceeding the predicted worst-case event value for the identified six mission lengths.

spectrum [*Tylka et al.*, 1997a]. In the given example, the proton flux/fluence has been converted to Fe flux/fluence; various outputs (probability of exceeding a given value, Fe fluence spectra) for different mission lengths are displayed in Figure 10 (bottom row). While the initial model outputs are created using the full set of 100,000 iterations for high resolution, the system only retains a set of 53 confidence levels from 50% to 99.9% for each channel and mission duration. Therefore, plots produced on this page display only this small subset of outputs at confidence intervals applicable for space applications.

All of the above functionality can instead be run on response functions created using the radiation effects tools available on SEPEM. The user can generate, for example, results of cumulative ionizing dose or maximum SEE rate for a given mission duration as a function of confidence or results for the time a certain effect rate is exceeded as a function of confidence level. These results are based on the derived effect time series rather than calculated from flux outputs from statistical models. This integrated functionality is unique to the SEPEM system.

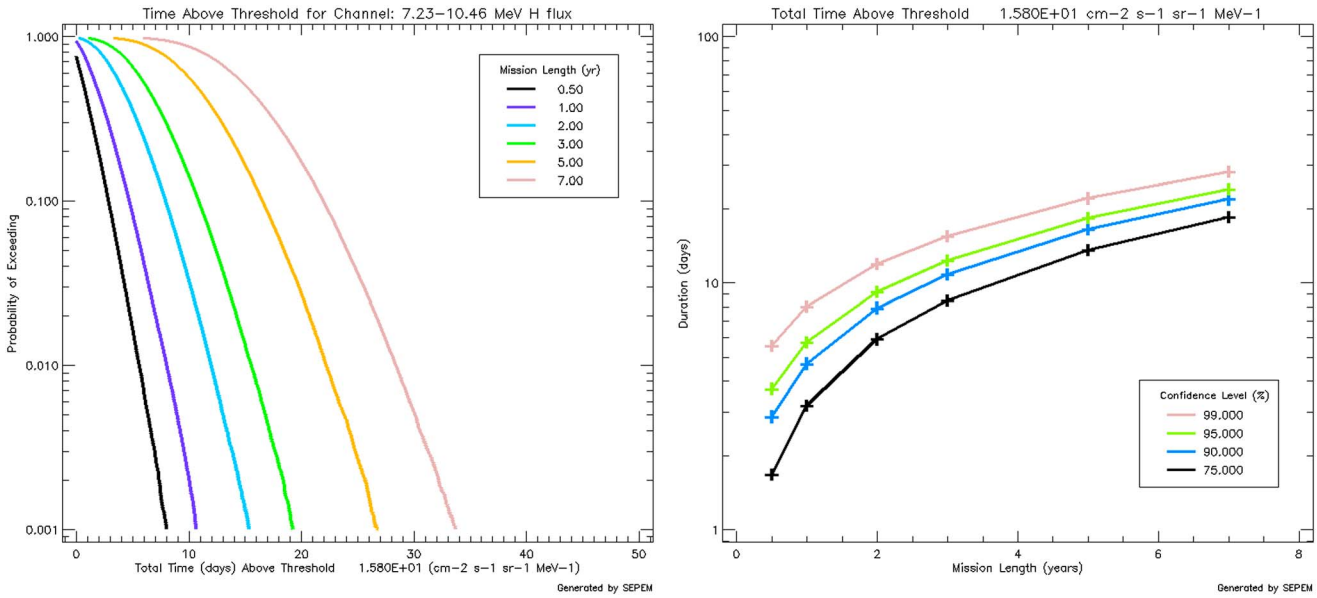

Figure 9. (left) The probability of exceeding the chosen threshold as a function of total time above threshold for six mission lengths. (right) The duration above the selected threshold value for various confidence levels as a function of mission length.

5. 0.2–1.6 AU Heliocentric Distance Analysis

SEPEM has recently gone a step further by providing the community a new tool (labeled as "Away from 1 AU modeling" in the SEPEM server left menu) to evaluate peak flux and fluence quantities for a spacecraft mission away from a heliocentric distance of 1 AU. The new method developed permits the inclusion in the previously described SEP statistical tools of outputs of a physics-based tool. This tool enables the prediction of the peak flux, worst-case event fluence, mission integrated fluence, and time above a threshold (contiguous worst case and mission total) between 0.2 AU and 1.6 AU in the ecliptic plane. The SOLar Particle ENgineering COde 2 (SOLPENCO2) tool was built under the SEPEM contract and is based on physical modeling of the proton intensity-time profiles of a number of gradual SEP reference events (six distinct types depending on their characteristics and solar origin, see below). By fitting the synthetic profiles of these reference events to observations at 1 AU, the synthetic profiles calculated for seven virtual observers located at different heliocentric radial distances (0.2, 0.4, 0.6, 0.8, 1.0, 1.3, 1.6 AU) and along the same nominal (Parker Spiral) interplanetary magnetic field line as the "1 AU observer" were calibrated. The resulting SEP peak fluxes and fluences, provided for the 10 SEPEM reference energy channels, were fitted for each enhancement as a function of the distance from the Sun to scaling laws covering the inner solar system [*Aran et al.*, 2011a].

The physical model underlying SOLPENCO2 [e.g., *Aran et al.*, 2011a, 2011b; *Jacobs and Poedts*, 2011; *Pomoell et al.*, 2015] combines 2-D MHD interplanetary shock propagation simulations developed during the SEPEM project with the particle transport code of *Lario et al.* [1998] to model proton intensity-time profiles of gradual SEP events. The new features of this shock-and-particle model that follows the same modular structure as previous models applied to single spacecraft and multispacecraft SEP events [e.g., *Aran et al.*, 2007] are as follows: (i) a solar wind model starting from 1.03 $R_\odot$ [*Jacobs and Poedts*, 2011], (ii) a simulation of the CME-driven shock tracked from 4 $R_\odot$ up to 1.6 AU, (iii) an automated method to detect the location of the shock front where a given observer is magnetically connected during the event, i.e., the observer's cobpoint ("Connecting with the OBserver POINT") [*Heras et al.*, 1995], and to compute the plasma variable ratios at the cobpoint, and (iv) the modeling of the transport of protons up to 200 MeV.

A semiempirical functional dependence between the plasma speed ratio across the shock, VR, and the injection rate of shock-accelerated protons, Q, at the cobpoint position, was established from the previous modeling of a number of SEP events [e.g., *Lario et al.*, 1998; *Aran et al.*, 2007, 2011a, 2011b; *Pomoell et al.*, 2015]. This relation, of the form $\log Q = \log Q_0 + k$ VR, permits the calculation of synthetic intensity-time profiles of SEP events for different virtual observers once VR is known through the MHD simulation of the

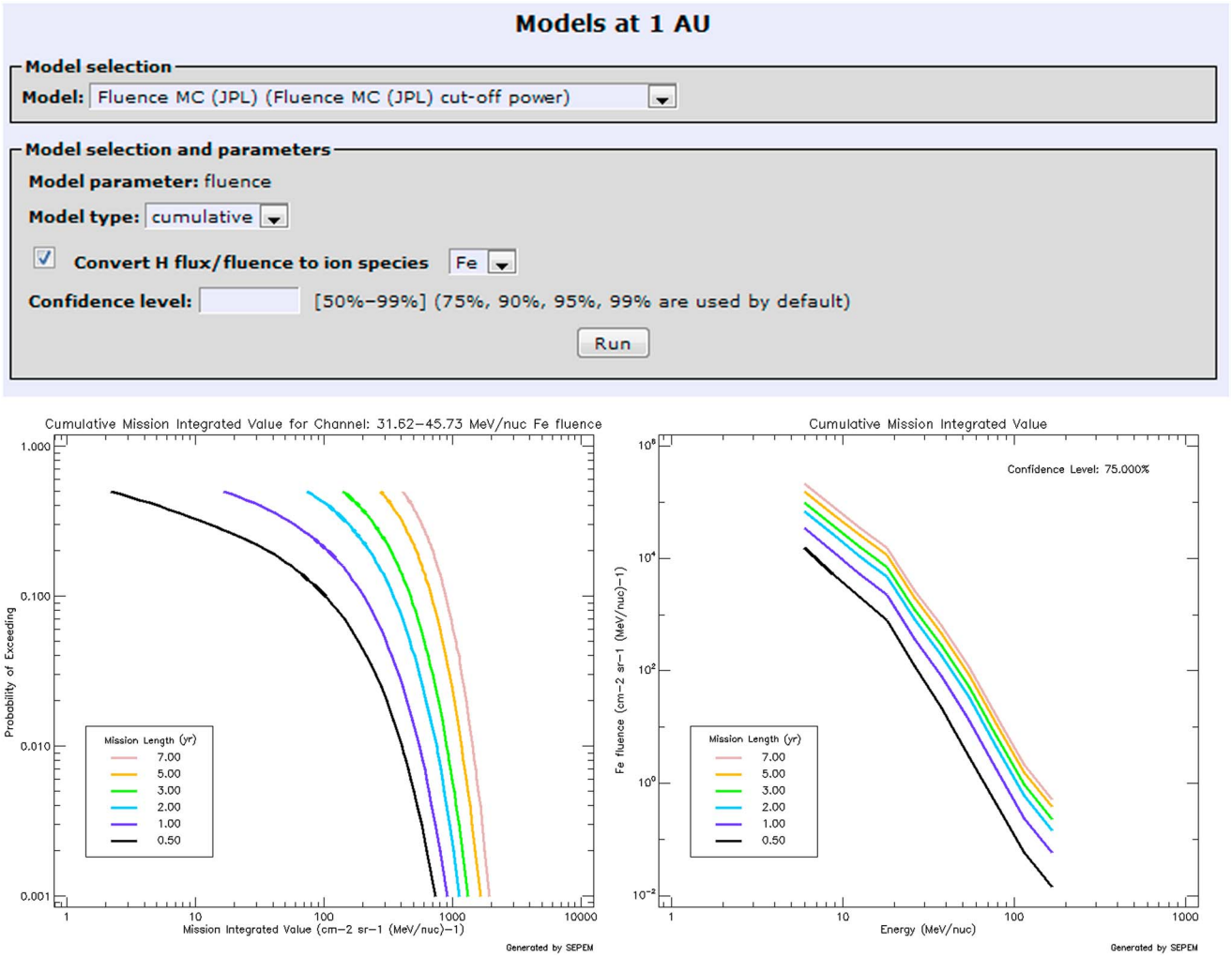

Figure 10. (top) "Models at 1 AU" form. (bottom left) Probability of exceeding a given Fe fluence value for a given mission length ranging from 0.5 year to 7 years. (bottom right) Fe energy spectra for the six mission lengths.

propagation of various interplanetary shocks and by assuming average values of the Q_0 and k parameters (see, for example, the SOLPENCO tool by *Aran et al.* [2006] and the works by *Aran et al.* [2011a, 2011b] and *Rodríguez-Gasén et al.* [2011, 2014]). The obtained Q is then introduced as input to the particle transport code [*Lario et al.*, 1998], and the upstream (i.e., until the shock arrival) proton intensity-time profiles for the observer of interest are obtained for the 10 SEPEM energy channels.

Six SEP enhancements were modeled following this procedure: the 4 April 2000 SEP event, the 6 and 10 June 2000 events, the 29 March 2001 event, and the two consecutive events on 13 and 14 December 2006. These enhancements were chosen to be representative of different types of SEP events seen in the SEPEM reference event list (see below for further details). In addition to model the near-Earth (i.e., 1 AU) observations of these events, we also calculate the proton intensity-time profiles for six other virtual observers distributed along the same interplanetary magnetic field line crossing the 1 AU observer and located at the radial distances specified above.

The synthetic peak intensity and event fluence values were scaled to the observed values at 1 AU in order to assure that the synthetic values match the reference data available for the statistical tools. Figure 11 shows one of the six SEP events modeled with SOLPENCO2, the 13 December 2006 SEP event. Figure 11 (left) displays the synthetic proton intensity-time profiles for three energy channels whose mean energy are 8.7, 26.3, and 115 MeV and for the seven observers placed at different radial distances (color coded). The

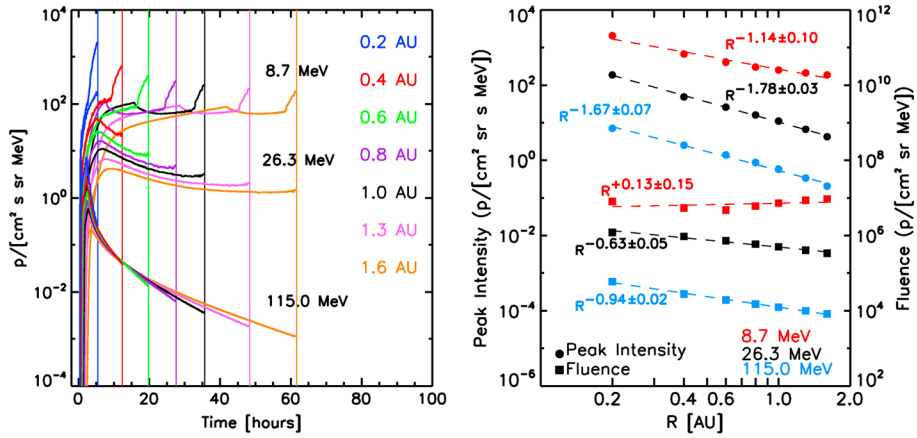

Figure 11. The 13 December 2006 SEP event. (left) Flux profiles at the simulated radial distances for 8.7 MeV, 26.3 MeV, and 115 MeV protons. (right) Peak intensity and event fluence variation with the radial distance of the observers.

vertical lines mark the shock passage by each of the observers. As can be seen in Figure 11 (left), SOLPENCO2 provides the synthetic profiles until the shock arrival at each observer; therefore, only upstream fluence is calculated from the synthetic profiles. In order to obtain the event fluence for each energy channel, we assume that the total-to-upstream fluence ratio determined from the observations at 1 AU is constant for all the virtual observers along the same interplanetary magnetic field line. The ratio applied to the synthetic events away from 1 AU is adopted for the sake of simplicity and due to the scarce amount of data available to validate these assumptions. It is a practical working assumption that permits the calculation of the event fluence, which is the fluence evaluated in the statistical calculations. The validation of this assumption and possible modification to the code is the scope of ongoing work.

Figure 11 (right) shows the variation of the peak intensity (circles) and of the event fluence (squares) with the heliocentric radial distance of the observers, *R*. To quantify this variation, a power law dependence of these magnitudes with *R* is assumed. The indices obtained depend on the energy of the protons and vary from event to event as observations have shown [e.g., *Lario et al.,* 2006, 2013]. This variation is mainly the result of the different conditions on the shock front scanned by the cobpoint and of how the magnetic connection is established in each case, that is, this variation also depends on the relative angular separation between the observer and the leading edge of the incoming interplanetary shock [see e.g., *Aran,* 2007; *Aran et al.,* 2011a; *Rodríguez-Gasén et al.*, 2011, 2014]. Other aspects that may explain the event to event and energy variations of the radial dependences observed in actual SEP events are the geometry of the shock and the seed particle population available [e.g., *Verkhoglyadova et al.,* 2012]. In SOLPENCO2, this latter feature is not considered (left for future model developments) and it is assumed that all particles are accelerated by the associated coronal/interplanetary shocks [see, e.g., *Pomoell et al.,* 2015].

The complexity of the SOLPENCO2 tool prevents the handling of it by a nonexpert user; and thus, it is not possible to make calls through the SEPEM server. Instead, the system provides the user with the plots of the particle energy spectra (peak flux and total fluence) for seven helioradial distances derived for the 135 events in the SEPEM reference event list covering the period from 1988 to 2007. These plots can be found in the left menu in the section "Away from 1 AU modeling," by selecting the "Event spectra" call. This 135 events list is labeled "the SEPEM radial dependent reference proton list."

As many SEP events in the SEPEM reference list are composed of multiple enhancements (sometimes called compound SEP events or episodes), there are in fact 204 SEP enhancements included in the 135 event list. In compound SEP events, the downstream region of one enhancement is overlapped by the onset of the following enhancement. The contributions of any remaining flux resulting from the first shock or of reacceleration by the following shock are included in the later enhancement. This method is aimed at giving an operative input for the statistical model until such a time that models which fully describe the physics involved in compound SEP events become available.

For each of these particle enhancements contained in the SEPEM radial dependent reference proton list, the solar origin, interplanetary shock passages, and particle intensity characteristics have been identified in order

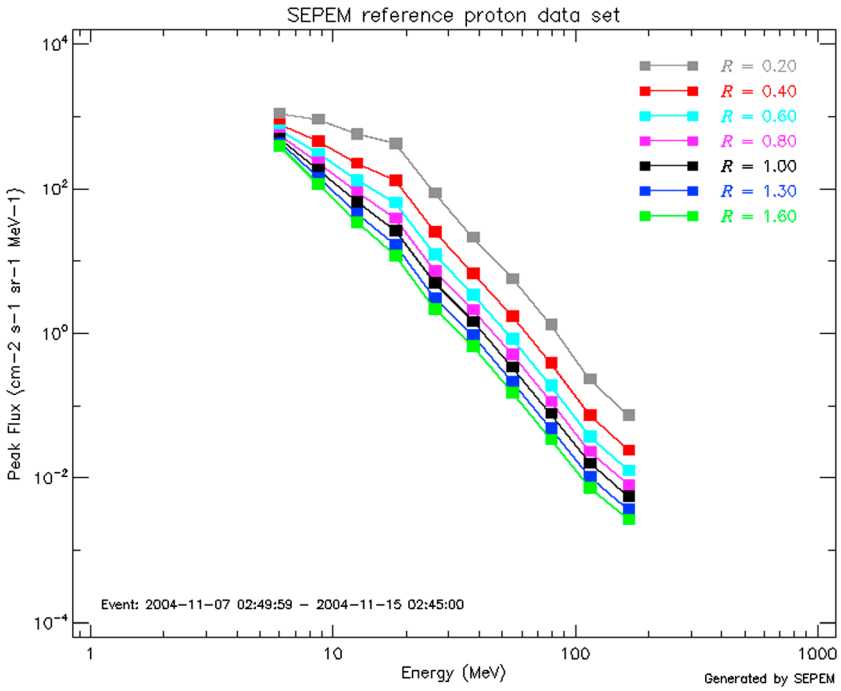

Figure 12. Peak flux event spectra of the 7–15 November 2004 event at the various SEPEM defined radial distances (0.2, 0.4, 0.6, 0.8, 1.0, 1.3, 1.6 AU) based on SOLPENCO2.

to classify these enhancements in terms of the six modeled reference types. Each enhancement was then assigned to the radial dependence corresponding to its type. It is clear that the classification of the natural extensive variety of SEP events into only six types is difficult because nature presents more than six types of SEP enhancements. This choice is a compromise resulting from the difficulty (and the CPU time needed) to model a particular SEP event and the desire to have a variety of reference cases to classify the remaining events (in the event list), as well as to furnish, for the first time, SEP statistical models with radial dependences that consider the contribution of traveling shocks to SEP events.

The methodology developed in SEPEM is a first attempt for achieving such a statistical model. It is clear that the more cases modeled, the more the radial dependent model would be improved. However, at present, the six reference cases allow the classification of SEP events according to (i) their association with interplanetary shock signatures at 1 AU; (ii) the detection of proton enhancements at high energies or not; (iii) the heliolongitude of their parent solar activity, and (iv) their peak intensity in the reference channel. More details of this classification are provided on the website at http://dev.sepem.oma.be/help/solpenco2_intro.html. Once the SEP enhancements are classified into one of the six reference types, the peak intensity and fluence spectra across radial distances can be computed based on the power law index of the reference enhancement and the scale given by the event fluxes measured at 1 AU, provided by the SEPEM reference event list. The result is an event list with an extra dimension for helioradial distance—the SEPEM radial dependent reference proton list. Figure 12 displays an example of the resulting peak flux event spectrum at the seven SEPEM radial distances (0.2, 0.4, 0.6, 0.8, 1.0, 1.3, 1.6 AU) for the 7–15 November 2004 compound SEP event.

Furthermore, the user is provided with the possibility of performing statistical analysis of the peak flux and fluence for missions with orbits between 0.2 AU and 1.6 AU by using the SEPEM radial dependent reference proton list. To achieve this, the system runs the model using Virtual Timelines as if it were at 1 AU, and when an event is randomly generated from the chosen distribution it is interpolated between the two closest distribution fits given the spacecraft position at that point in time, by using a single randomly generated probability applied to each flux distribution. At present, these analyses are limited to peak flux and fluence applied to the SEPEM radial dependent event list. To use another list would require the SOLPENCO2 tool to be run dynamically which is not feasible at present. More details on the method applied to include the radial dependent information into the statistical modeling are described here http://dev.sepem.oma.be/help/solpenco2_intro.html.

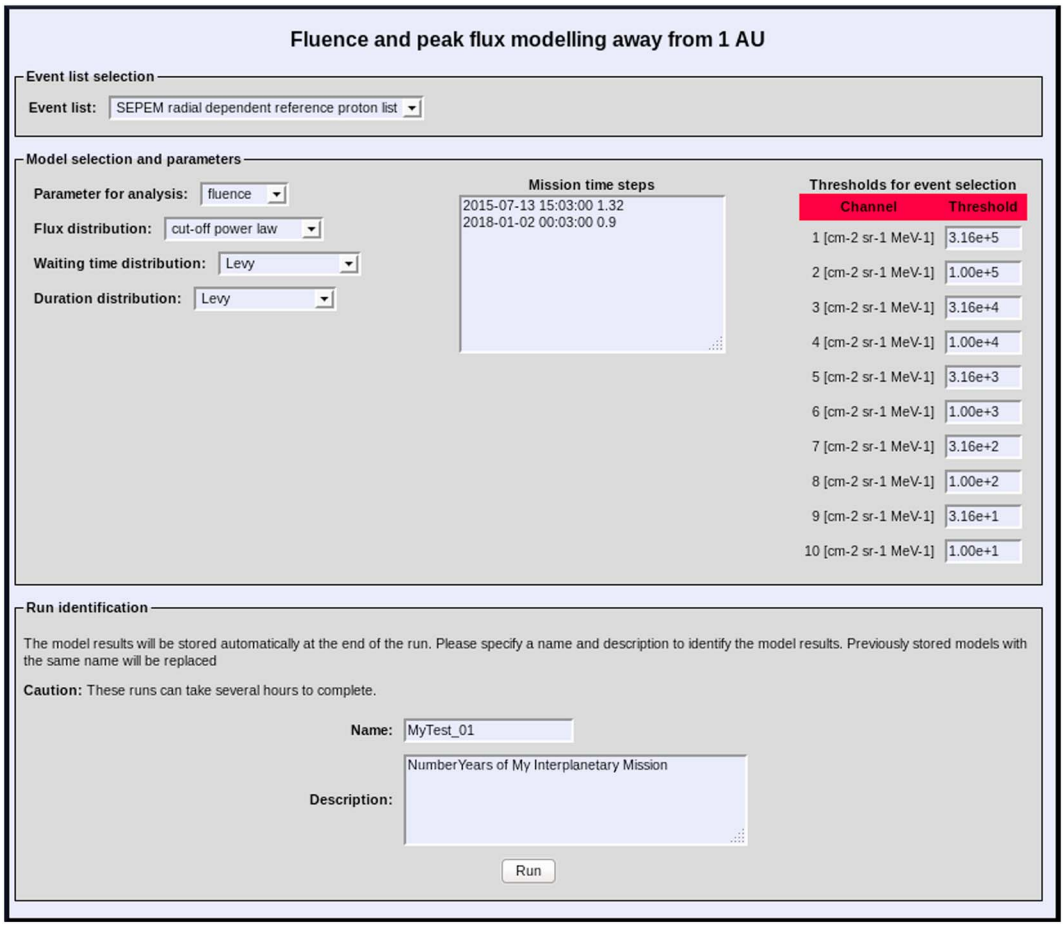

Figure 13. SEPEM interface for statistical modeling of fluence and peak flux for interplanetary missions.

Figure 13 shows the system interface for the SEP radial dependent statistical tool that appears when selecting "Fluence and peak intensity" in the left menu. The user has to provide the desired orbit (date, time, and radial distance from the Sun in AU) in the "Mission time steps" box and select the statistical methods to be applied (Table 2). The user can also specify intensity thresholds for determining the SEP events, otherwise default values are given by the system, as shown in Figure 13. A help page describing how to use this tool appears when selecting "context help" in the right menu.

The outputs of the model allow the user to compare the results for three different possibilities regarding the radial distance scaling: (i) no distance dependence, (ii) the ECSS-E-ST-10-04C (https://www.spenvis.oma.be/ecss/frame.php/e_st_10_04c and http://www.ecss.nl/) recommendation of r^{-2} for helioradial distances < 1 AU, and (iii) the output based on SOLPENCO2 (i.e., the SEPEM method for distance scaling). Here we present an example for an interplanetary mission operating during 20.01 years, starting on 1 January 2014. Figure 14 shows the radial distances (in AU, right vertical axis) covered by the entire mission (black curve). Asterisks mark the positions of the spacecraft specified by the user, and the height of each block represents the scaled fluence (in $cm^{-2}\,sr^{-1}\,MeV^{-1}$, left vertical axis). Note that the temporal axis of the plot does not coincide with the mission timescale, but with entire periods of solar maximum (red blocks) or solar minimum (blue blocks) in order to ensure that plots can be read regardless of the duration of mission provided. For missions in the future, the current solar maximum date is repeated with an 11 year cycle.

The duration of this mission has been divided in different mission lengths (2.00, 4.01, 7.00, 4.01, and 3.00 years) for which the spacecraft moves within a broad range of distances from the Sun to showcase the effect on the accumulated fluence of the radial position of the spacecraft. In Figure 14, the cumulative fluence is shown, for a 90% confidence level and for 66.13—95.64 MeV protons. In this case, the fluence is obtained applying the SEPEM method for radial scaling. It is seen that in those periods of equal duration

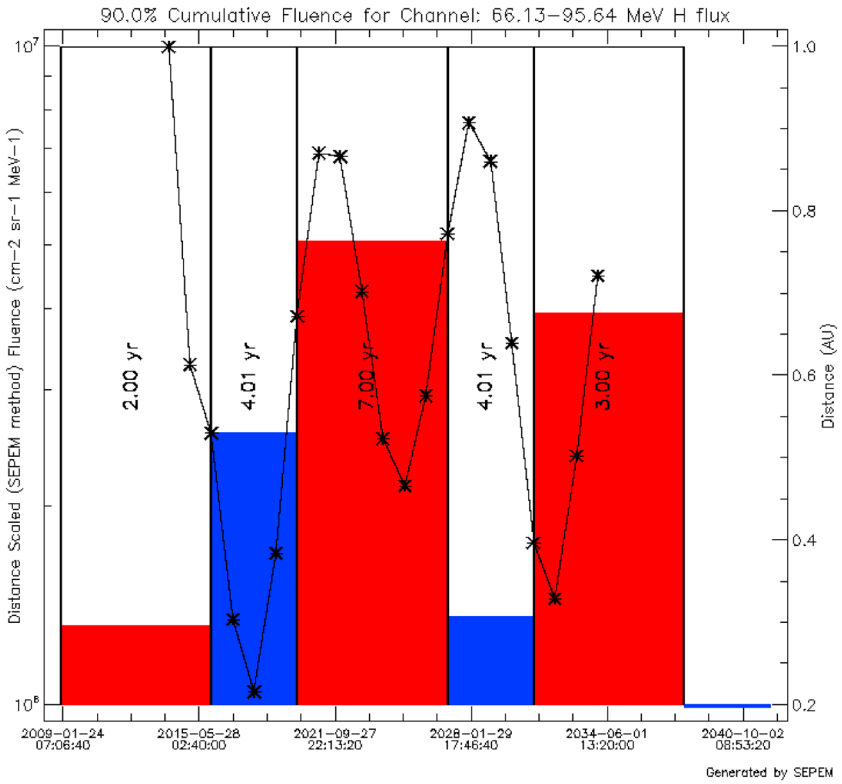

Figure 14. Proportion of the fluence contributed by each of the five periods in which a 20.01 years mission has been divided. Maximum periods of the solar cycles are shown in red and minimum in blue. Fluence values are obtained with 90% confidence level. Overlaid in black is the mission orbit, where asterisks mark the mission steps specified by the user.

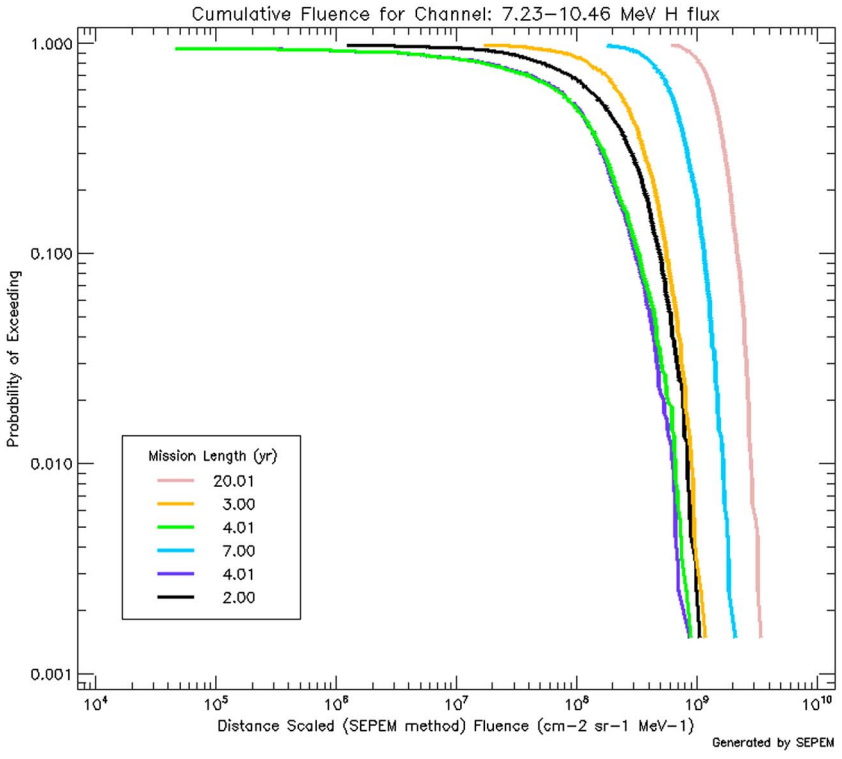

Figure 15. Probability of exceeding a certain value of cumulative fluence for 7.23–10.46 MeV protons. Curves are displayed for each period of time (in years) into which the mission has been divided (color coded) and for the total mission length (pink curve).

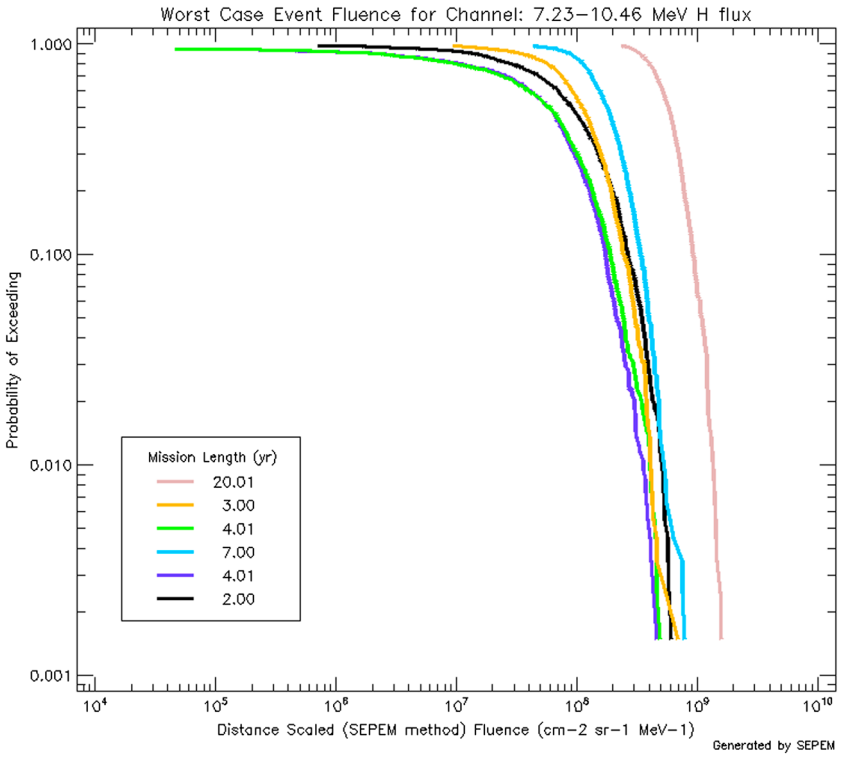

Figure 16. Probability of exceeding a certain value of 7.23–10.46 MeV protons fluence for the worst-case event fluence assumption. Curves are displayed for each period of time (in years) into which the mission has been divided (color coded) and for the total mission length (pink curve).

and solar cycle phase, the fluence is larger when the spacecraft is close to the Sun (i.e., first 4 years blue block, solar minimum cruise) than when it is moving far from it (i.e., the second 4 years blue block). As expected, the larger values of accumulated fluence correspond to solar cycle maximum periods. Figure 15 shows model outputs for the probability of exceeding a certain value of fluence calculated by using the radial distance scaling as derived from SOLPENCO2 (i.e., the SEPEM method for distance scaling). These probability curves show the cumulative fluence for 7.23—10.46 MeV protons and for the same five phases of various lengths into which the orbit has been divided. Results corresponding to the total mission length are also displayed (pink curve). Figure 16 shows the same probability curves but for the results of the worst-case event fluence. In this simulated mission, larger values of cumulative fluence can be exceeded more easily for longer periods during solar maximum phases, whereas in the case of the worst-case event fluence, closer values of maximum fluence are reached among the different mission phases considered.

6. Summary

With the launch of the SEPEM application server, the community (scientists, spacecraft designers, spacecraft operators, etc.) has been equipped with a unique system that provides an implementation of several well-known modeling methodologies, built on long-term cleaned data sets and an increased understanding of the SEP event process. It also allows the plotting and inspection of raw, processed and shielded time series data for scientific and operations support.

SEPEM gives the user increased flexibility in his/her analysis and allows generation of mission integrated fluence statistics, peak flux statistics, and other functionalities. Both statistical and physical modeling techniques have been addressed in the SEPEM project, covering not only 1 AU heliocentric distance but also SEP environments ranging from 0.2 AU to 1.6 AU using the newly developed physics-based SOLPENCO2 tool to simulate particle flux profiles of gradual SEP events. This new method provides the user with a statistical tool to evaluate peak flux and fluence quantities for spacecraft missions in the inner solar system. SEPEM moves beyond mission integrated fluence statistics to peak flux statistics and

durations of high flux periods. SEPEM has also integrated effects tools to allow calculation of single event upset rate and investigation of the effect of shielding for a variety of engineering scenarios; the statistical methods can also be applied to these effects parameters.

An extensive set of help pages is available on the SEPEM application server, including background material, information on the data sets and processing, and context sensitive help for each application page. Use of SEPEM is free of charge, but registration is required and can be done from the homepage (http://dev.sepem.oma.be/).

SEPEM has resulted in several follow-on projects including as follows: Interplanetary and Planetary Radiation Modelling for Human Spaceflight—an ESA activity investigating the effect of SEP events on humans on EVA and behind thick shielding which necessitates an extension of the proton data range using ground-based neutron monitor data sets (project led by DH Consultancy, Belgium, completed in January 2015); SEPCALIB—a thorough investigation into the automated calibration algorithms used in SEPEM to validate the output processed data sets and recommend updates to the data processing chain (work undertaken by the Institute of Accelerating Systems and Applications (IASA), Greece, completed in July 2014) [see *Sandberg et al.,* 2014]; and Energetic Solar Heavy Ion Environment Models—an extension and update of the SEPEM system to include processed heavy ion data, code for attenuating particles due to geomagnetic shielding for Earth-orbiting spacecraft below geostationary and a fast shielding propagation tool capable of combining all relevant SEP species in a single analysis (ongoing project led by Kallisto Consultancy, UK). Furthermore, the EU FP7 Coronal Mass Ejections and Solar Energetic Particles project, led by the Belgian Institute for Space Aeronomy, used the SEPEM reference proton data set and event list for its statistical analyses, see http://comesep.aeronomy.be/.

The ESA SEPEM first prototype project was developed by an international consortium (Belgian Institute for Space Aeronomy, Belgium, Project Lead; K.U.Leuven, Belgium; QinetiQ, UK; University of Barcelona, Spain; University of Southampton, UK; Mars Space Ltd, UK; and DH Consultancy, Belgium). For further information please contact the Project Manager N. Crosby.

Acknowledgments

This study was performed under the TRP (Technology Research Programme) ESA contract 20162/06/NL/JD. Àngels Aran and Blai Sanahuja were also partially supported by the Spanish Ministerio de Economía y Competitividad, under the projects AYA2010-17286 and AYA2013-42614-P. Computational support was also provided by the Consorci de Serveis Universitaris de Catalunya (CSUC). The authors would like to acknowledge Mike Xapsos for providing his data set for comparison purposes and for discussions about the statistical models. Also, thanks go to the reviewers of this paper whose feedback helped improve the overall message that this paper aims to convey regarding SEPEM and its various functions.

References

Agostinelli, S., et al. (2003), Geant4—A simulation toolkit, *Nucl. Instrum. Methods Phys. Res.*, *506*, 250–303.

Allison, J., et al. (2006), Geant4 developments and applications, *IEEE Trans. Nucl. Sci.*, *53*(1), 270–278.

Aran, A. (2007), Synthesis of proton flux profiles of SEP events associated with interplanetary shocks. The tool SOLPENCO, PhD thesis, Universitat de Barcelona. [Available at http://www.am.ub.edu/~blai/articles/Aran_thesis.pdf.]

Aran, A., B. Sanahuja, and D. Lario (2006), SOLPENCO: A solar particle engineering code, *Adv. Space Res.*, *37*, 1240–1246.

Aran, A., D. Lario, B. Sanahuja, R. G. Marsden, M. Dryer, C. D. Fry, and S. M. P. McKenna-Lawlor (2007), Modeling and forecasting solar energetic particle events at Mars: The event on 6 March 1989, *Astron. Astrophys.*, *469*, 1123–1134.

Aran, A., P. Jiggens, B. Sanahuja, C. Jacobs, D. Heynderickx, and D. Lario (2011a), Developing a new model for gradual SEP events: Peak intensities and fluences within 1.6 AU, Abstract SH33B-2051 presented at 2011 AGU Fall Meeting, AGU, San Francisco, Calif.

Aran, A., C. Jacobs, R. Rodríguez-Gasén, B. Sanahuja, and S. Poedts (2011b), WP410: Initial and boundary conditions for the shock-and-particle model, *SEPEM Tech. Rep.*, ESA/ESTEC Contract 20162/06/NL/JD, 1–58. [Available at http://www.am.ub.edu/~blai/articles/Aran_etal_2011_SEPEM_TN_WP410.pdf.]

Baker, D. N., J. E. Mazur, and G. Mason (2012), SAMPEX to reenter atmosphere: Twenty-year mission will end, *Space Weather*, *10*, S05006, doi:10.1029/2012SW000804.

Band, D., et al. (1993), Batse observations of gamma-ray burst spectra. I—Spectral diversity, *Astrophys. J.*, *413*(1), 281–292.

Crosby, N. (2009), Solar extreme events 2005–2006: Effects on near-Earth space systems and interplanetary systems, *Adv. Space Res.*, *43*(4), 559–564.

Crosby, N. B., V. Bothmer, R. Facius, J.-M. Griessmeier, X. Moussas, M. Panasyuk, N. Romanova, and P. Withers (2008), Interplanetary space weather and its planetary connection, *Space Weather*, *6*, S01003, doi:10.1029/2007SW000361.

Cucinotta, F. A., S. Hu, N. A. Schwadron, K. Kozarev, L. W. Townsend, and M.-H. Y. Kim (2010), Space radiation risk limits and Earth-Moon-Mars environmental models, *Space Weather*, *8*, S00E09, doi:10.1029/2010SW000572.

DiGregorio, B. E. (2008), Surviving the Sun's wrath at Mercury: The MESSENGER mission, *Space Weather*, *6*, S03003, doi:10.1029/2008SW000386.

Dodd, P. E., and L. W. Massengill (2003), Basic mechanisms and modeling of single-event upset in digital microelectronics, *IEEE Trans. Nucl. Sci.*, *50*, 583–602.

ECSS-E-HB-10-12A (2010), Space engineering—Calculation of radiation and its effects and margin policy handbook, European Cooperation for Space Standardization (ECSS), ESA Requirements and Standards Division.

Feynman, J., and S. B. Gabriel (2000), On space weather consequences and predictions, *J. Geophys. Res.*, *105*(A5), 10,543–10,564, doi:10.1029/1999JA000141.

Feynman, J., T. P. Armstrong, L. Dao-Gibner, and S. Silverman (1990), A new interplanetary fluence model, *J. Spacecr. Rockets*, *27*(4), 403–410.

Feynman, J., G. Spitale, J. Wang, and S. B. Gabriel (1993), Interplanetary proton fluence model: JPL 1991, *J. Geophys. Res.*, *98*(A8), 13,281–13,294, doi:10.1029/92JA02670.

Feynman, J., A. Ruzmaikin, and V. Berdichevsky (2002), The JPL proton fluence model: An update, *J. Atmos. Sol. Terr. Phys.*, *64*(16), 1679–1686.

Glover, A., A. Hilgers, L. Rosenqvist, and S. Bourdarie (2008), Interplanetary proton cumulated fluence model update, *Adv. Space Res.*, *42*(9), 1564–1568.

Gopalswamy, N., S. Yashiro, G. Stenborg, and R. Howard (2003), Coronal and interplanetary environment of large solar energetic particle events, in Proceedings of 28th International Cosmic Ray Conference, Universal Academy Press, Inc., 3549–3552.

Heras, A. M., B. Sanahuja, D. Lario, Z. K. Smith, T. Detman, and M. Dryer (1995), Three low-energy particle events: Modeling the influence of the parent interplanetary shock, *Astrophys. J.*, *445*, 497–508.

International Commission on Radiation Units and Measurements (ICRU) (2005), International commission on radiation units and measurements, stopping of ions heavier than helium, ICRU Rep. 73, J. ICRU 5(1), Oxford Univ. Press, Oxford, U. K.
Jacobs, C., and S. Poedts (2011), A polytropic model for the solar wind, *Adv. Space Res.*, *48*, 1058.
Jiggens, P. T. A., and S. B. Gabriel (2009), Time distributions of solar energetic particle events: Are SEPEs really random?, *J. Geophys. Res.*, *114*, A10105, doi:10.1029/2009JA014291.
Jiggens, P. T. A., S. B. Gabriel, D. Heynderickx, N. B. Crosby, A. Glover, and A. Hilgers (2012), ESA SEPEM project: Peak flux and fluence model, *IEEE Trans. Nucl. Sci.*, *59*, 4.
Jiggens, P. T. A., M.-A. Chavy-Macdonald, G. Santin, A. Menicucci, H. Evans, and A. Hilgers (2014), The magnitude and effects of extreme solar particle events, *J. Space Weather Space Clim.*, *4*.
Lario, D., B. Sanahuja, and A. M. Heras (1998), Energetic particle events: Efficiency of interplanetary shocks as 50 keV $<$ E $<$ 100 MeV proton accelerators, *Astrophys. J.*, *509*, 415–434.
Lario, D., M.-B. Kallenrode, R. B. Decker, E. C. Roelof, S. M. Krimigis, A. Aran, and B. Sanahuja (2006), Radial and longitudinal dependence of solar 4–13 MeV and 27–37 MeV proton peak intensities and fluences: Helios and IMP 8 observations, *Astrophys. J.*, *653*(2), 1531–1544.
Lario, D., A. Aran, R. Gómez-Herrero, N. Dresing, B. Heber, G. C. Ho, R. B. Decker, and E. C. Roelof (2013), Longitudinal and radial dependence of solar energetic particle peak intensities: STEREO, ACE, SOHO, GOES, and MESSENGER observations, *Astrophys. J.*, *767*, 41–58, doi:10.1088/0004-637X/767/1/41.
Lei, F. (2007), REAT-MS project: Implementation of a simple charge collection mechanism in the GEMAT code, QinetiQ Tech. Rep. QinetiQ/S&DU/Space/TR0700301.
Lei, F., and P. Truscott (2007), Radiation effects on advanced technologies—Models and software (REAT-MS) contract final report, QinetiQ Customer Rep., QINETIQ/EMEA/S&DU/CR0708251.
Lei, F., et al. (2002), MULASSIS: A Geant4-based multilayered shielding simulation tool, *IEEE Trans. Nucl. Sci.*, *49*, 2788–2793.
Luhmann, J. G., S. A. Ledvina, D. Odstrcil, M. J. Owens, X.-P. Zhao, Y. Liu, and P. Riley (2010), Cone model-based SEP event calculations for applications to multipoint observations, *Adv. Space Res.*, *46*, 1–21.
Luo, P. and J. Zhang (2011), SEU mitigation strategies for SRAM-based FPGA, Proc. SPIE 8196, International Symposium on Photoelectronic Detection and Imaging 2011: Space Exploration Technologies and Applications, doi:10.1117/12.899744.
Maris, O., and N. B. Crosby (2012), Space environment effects on space- and ground-based technological systems, in *Advances in Solar and Solar-Terrestrial Physics*, edited by G. Maris, and C. Demetrescu, pp. 293–328, Research Signpost, Kerala, India.
Mason, G. M., J. E. Mazur, J. R. Dwyer, J. R. Jokipii, R. E. Gold, and S. M. Krimigis (2004), Abundances of heavy and ultraheavy ions in 3He-rich solar flares, *Astrophys. J.*, *606*(1), 555–564, doi:10.1086/382864.
McGuire, R. E., T. T. von Rosenvinge, and F. B. McDonald (1986), The composition of solar energetic particles, *Astrophys. J.*, *301*, 938.
Mewaldt, R. A., M. D. Looper, C. M. S. Cohen, G. M. Mason, D. K. Haggerty, M. I. Desai, A. W. Labrador, R. A. Leske, and J. E. Mazur (2005), Solar-particle energy spectra during the large events of October-November 2003 and January 2005, *Proceedings of the 29th International Cosmic Ray Conference*, 1-101-104.
Mewaldt, R. A., et al. (2010), Record-setting cosmic-ray intensities in 2009 and 2010, *Astrophys. J. Lett.*, *723*, L1–L6.
O'Neill, P. M. (2010), Badhwar–O'Neill 2010 galactic cosmic ray flux model—Revised, *IEEE Trans. Nucl. Sci.*, *57*, 6.
Onsager, T. G., R. Grubb, J. Kunches, L. Matheson, D. Speich, R. Zwickl, and H. Sauer (1996), Operational uses of the GOES energetic particle detectors, in *SPIE Conference Proceedings, GOES-8 and Beyond*, vol. 2812, edited by E. R. Washwell, pp. 281–290, SPIE, Denver, Colo.
Petersen, E. (1997), Single event analysis and prediction, IEEE Nuclear and Space Radiation Effects Conference, Short Course section III.
Pomoell, J., A. Aran, C. Jacobs, R. Rodríguez-Gasén, S. Poedts, and B. Sanahuja (2015), Modelling large solar proton events with the shock-and-particle model, *J. Space Weather Space Clim.*, *5*, A12, doi:10.1051/swsc/2015015.
Rodriguez, J. V., J. C. Krosschell, and J. C. Green (2014), Intercalibration of GOES 8–15 solar proton detectors, *Space Weather*, *12*, 92–109, doi:10.1002/2013SW000996.
Rodríguez-Gasén, R., A. Aran, B. Sanahuja, C. Jacobs, and S. Poedts (2011), Why should the latitude of the observer be considered when modeling gradual proton events? An insight using the concept of cobpoint, *Adv. Space Res.*, *47*, 2140–2151, doi:10.1016/j.asr.2010.03.021.
Rodríguez-Gasén, R., A. Aran, B. Sanahuja, C. Jacobs, and S. Poedts (2014), Variation of proton flux profiles with the observer's latitude in simulated gradual SEP events, *Sol. Phys.*, *289*, 1745–1762, doi:10.1007/s11207-013-0442-1.
Rosenqvist, L., and A. Hilgers (2003), Sensitivity of a statistical solar proton fluence model to the size of the event data set, *Geophys. Res. Lett.*, *30*(16), 1865, doi:10.1029/2003GL017038.
Rosenqvist, L., A. Hilgers, H. Evans, E. Daly, M. Hapgood, R. Stamper, R. Zwickl, S. Bourdarie, and D. Bosher (2005), A toolkit for updating interplanetary proton cumulated fluence models, *J. Spacecr. Rockets*, *42*, 6.
Sandberg, I., P. Jiggens, D. Heynderickx, and I. A. Daglis (2014), Cross calibration of NOAA GOES solar proton detectors using corrected NASA IMP-8/GME data, *Geophys. Res. Lett.*, *41*, 4435–4441, doi:10.1002/2014GL060469.
Sellers, F. B., and F. A. Hanser (1996), Design and calibration of the GOES-8 particle sensors: The EPS and HEPAD, in *Proc. SPIE, GOES-8 and Beyond*, vol. 2812, edited by E. R. Washwell, pp. 353–364, SPIE, Denver, Colo.
Sigmund, P., A. Schinner, and H. Paul (2009), Errata and addenda for ICRU report 73, *J. ICRU*, *5*, 1.
Tretkoff, E. (2010), Space weather and satellite engineering: An interview with Michael Bodeau, *Space Weather*, *8*, S03003, doi:10.1029/2010SW000584.
Tylka, A. J., J. H. Adams, P. R. Boberg, B. Brownstein, W. F. Dietrich, E. O. Flueckiger, E. L. Petersen, M. A. Shea, D. F. Smart, and E. C. Smith (1997a), CREME96: A revision of the cosmic ray effects on micro-electronics code, *IEEE Trans. Nucl. Sci.*, *44*, 2150–2160.
Tylka, A. J., W. F. Dietrich, and P. R. Boberg (1997b), Probability distributions of high-energy solar-heavy-ion fluxes from IMP-8: 1973–1996, *IEEE Trans. Nucl. Sci.*, *44*(6), 2140–2149.
Vainio, R., et al. (2009), Dynamics of the Earth's particle radiation environment, *Space Sci. Rev.*, *147*, 187–231, doi:10.1007/s11214-009-9496-7.
Verkhoglyadova, O. P.,G. Li, X. Ao, G. P. Zank (2012), Radial dependence of peak proton and iron ion fluxes in solar energetic particle events: Application of the PATH code, *Astrophys. J.*, *757*(1), 75, doi:10.1088/0004-637X/757/1/75.
Xapsos, M. A., G. P. Summers, and E. A. Burke (1998), Extreme value analysis of solar energetic proton peak fluxes, *Solar Phys.*, *183*, 157–164.
Xapsos, M. A., G. P. Summers, J. L. Barth, E. G. Stassinopoulos, and E. A. Burke (1999), Probability model for worst case solar proton event fluences, *IEEE Trans. Nucl. Sci.*, *46*(6), 1481–1485.
Xapsos, M. A., G. P. Summers, J. L. Barth, E. G. Stassinopoulos, and E. A. Burke (2000), Probability model for cumulative solar proton event fluences, *IEEE Trans. Nucl. Sci.*, *47*(3), 486–490.
Xapsos, M. A., C. Stauffer, G. B. Gee, J. L. Barth, E. G. Stassinopoulos, and R. E. McGuire (2004), Model for solar proton risk assessment, *IEEE Trans. Nucl. Sci.*, *51*(6), 3394–3398.